Journal of Electrical Engineering and Computer (JEECOM)
Vol. 8, No. 2 (2026), DOI: 10.33650/jeecom.v8i2.17186
P-ISSN: 2715-0410; E-ISSN: 2715-6427

Quantifying Overhaul Effectiveness for a 6 kV Primary Air Fan Motor: A Multi-Parameter Diagnostic Assessment against International Standards

Elih Mulyana[1*], Pambudi Nur Hafizh[2], Muhamad Habibi[3]
[1]Professional Engineer Program, Universitas Pendidikan Indonesia, Bandung, Indonesia
[2]Department of Electrical Engineering, Universitas Pendidikan Indonesia, Bandung, Indonesia
[3]Institut Teknologi PLN, Jakarta, Indonesia

Article Info

Article history:
Received August 29, 2026
Revised September 8, 2026
Accepted September 10, 2026

Keywords:
PA Fan motor
Condition assessment
Overhaul
Insulation resistance
Vibration
IEEE Std 43-2013
ISO 20816-3

ABSTRACT

Reliability of 6 kV auxiliary motors is critical to combustion stability in coal-fired steam power plants, yet the quantified effectiveness of overhaul interventions on such motors is seldom reported. This study evaluates a 6 kV Primary Air Fan (PA Fan) induction motor through multi-parameter diagnostics performed during a scheduled overhaul, covering insulation resistance, winding-resistance unbalance, bearing vibration, and mechanical clearance, referenced to IEEE Std 43-2013, ISO 20816-3, IEC 60034-1, NEMA MG 1, and the manufacturer design tolerances. Vibration under load decreased by 49.1% in the vertical direction at the non-drive-end (NDE) bearing, and the mean of the six load-condition readings fell by 20.5% (2.13 to 1.69 mm/s), correlating with the equalization of the NDE bearing top clearance (0.19/0.32 to 0.23/0.22 mm), which indicates that the dominant benefit of the overhaul for this motor was mechanical. Winding-resistance unbalance was 0.279%, far below the 2% acceptance limit. The post-cleaning drop in absolute insulation resistance is consistent with measurement on a warm winding after the running test; as winding temperature was not recorded, insulation integrity is confirmed by the ratio-based Dielectric Absorption Ratio (DAR, 1.62) and Polarization Index (PI, 2.39) rather than by absolute comparison. All measured parameters comply with their applicable acceptance criteria, and the motor is deemed fit for continued operation. The study quantifies overhaul effectiveness and illustrates, on a field case, the consequence of omitting the temperature normalization required by IEEE Std 43-2013: a legitimate maintenance action can be misread as dielectric degradation.

Corresponding Author:
Elih Mulyana,
Professional Engineer Program, Universitas Pendidikan Indonesia, Bandung, Indonesia.
Email: elihmulyana@upi.edu; Orchid Id: https://orcid.org/0000-0002-3253-9372

1. INTRODUCTION

Coal-fired steam power plants (Pembangkit Listrik Tenaga Uap, PLTU) remain the backbone of the Indonesian national electricity system, and their reliability depends heavily on the health of the auxiliary equipment that sustains the combustion process [1], [2]. As the national generation mix absorbs a growing share of variable renewable capacity, subcritical coal units in Indonesia — including the plant examined here — are increasingly required to operate flexibly rather than at a fixed base load [1], which raises both the duty cycle and the number of start–stop transients imposed on their auxiliary drives. Among the most critical of these drives is the medium-voltage Primary Air Fan (PA Fan) induction motor, which supplies pressurized primary air to transport pulverized coal from the coal mill to the burner; instability of this motor directly affects the air–fuel ratio, combustion quality, and boiler efficiency. The 6 kV motor driving the PA Fan operates under high dynamic load and, during Direct-on-Line (DOL) starting, draws a starting current several times the rated value while the air-gap flux is established abruptly; the resulting transient electromagnetic torque oscillations are transmitted through the shaft and the bearing housings as mechanical vibration, and the repetition of these transient stresses over successive starts accelerates bearing and insulation wear [3], [4]. Because an unplanned failure of this motor can force unit derating or shutdown, its electrical and mechanical integrity must be preserved through a measurable maintenance program.

The diagnosis of induction motors has matured into a distinct discipline combining offline testing and online monitoring. In the electrical domain, the integrity of stator-winding insulation is evaluated through insulation-resistance testing, the Dielectric Absorption Ratio (DAR), and the Polarization Index (PI) in accordance with IEEE Std 43-2013 [5], which stresses that insulation-resistance values must be normalized to a 40 °C reference temperature to be validly comparable; without this correction, cross-condition comparison is prone to error owing to the sensitivity of insulation to temperature and humidity [6], [7]. Advanced methods such as Motor Current Signature Analysis (MCSA) enable early detection of rotor faults, broken bars, and eccentricity through spectral analysis of the stator current without stopping the machine [8], [9], while comprehensive reviews of induction-motor condition monitoring map the relationship between fault types — winding, bearing, rotor, and eccentricity — and their diagnostic signatures [10]. In the mechanical domain, rolling-element bearing diagnosis through vibration analysis is methodologically well established [11], [12], [13], with vibration severity assessed against the ISO 20816-3 zone criteria [14].

In power-plant maintenance practice, periodic overhaul is the principal instrument for restoring components to optimal condition through inspection, cleaning, repair, and calibration. The maintenance paradigm has shifted from time-based toward condition-based and predictive approaches that assess machine health from actual data and degradation trends, enabling timely intervention and minimizing unplanned shutdowns [15], [16], [17]. Condition-based monitoring of induction motors is increasingly supported by intelligent instrumentation for continuous parameter acquisition [18], and field studies show that correct insulation-resistance testing improves the interpretation of three-phase motor performance [19]. Recent multi-parameter assessments of aging induction motors likewise combine insulation, winding-resistance, and vibration diagnostics within a single evaluation campaign [20]. The same evidence-based orientation is visible more broadly in contemporary power-and-instrumentation engineering: decisions on how an asset should be operated or maintained are increasingly derived from measured system data rather than from fixed schedules, whether the object is a distribution network whose load dispatch is optimized against price and demand signals [21] or an instrumentation system whose performance claims are established by evaluation in the field rather than in the laboratory [22]. The present work adopts that same posture for a rotating-machine overhaul. Nevertheless, most of the literature stops at a binary statement of compliance against a threshold and has not systematically quantified how much a given overhaul action improves a particular parameter.

Although standard-referenced acceptance testing of high-voltage motors is well documented, the literature seldom reports the quantified effectiveness of individual overhaul interventions on multi-parameter measurements, nor does it systematically address the post-cleaning insulation-resistance anomaly frequently observed in the field — an anomaly that may be misinterpreted as dielectric degradation when temperature normalization per IEEE Std 43-2013 is not applied. This gap motivates a field-based case study that does not merely declare fitness but quantifies the magnitude of improvement and interprets diagnostic anomalies on a physical basis.

Accordingly, the objectives of this study are to: (1) quantify the effectiveness of the overhaul on the mechanical parameters, and establish the standing of the electrical parameters, of a 6 kV PA Fan motor; (2) analyze the post-cleaning insulation-resistance behavior and its implications for the validity of pre-/post-overhaul comparison; and (3) assess the motor's fitness for operation against IEEE Std 43-2013, ISO 20816-3, IEC 60034-1, and the manufacturer design tolerances. The main contribution of this article is a multi-parameter diagnostic assessment that quantifies overhaul effectiveness and shows, on a field case, what follows from omitting the temperature normalization that IEEE Std 43-2013 requires — a correct maintenance action may be misdiagnosed as a failure — while providing one documented data point for the condition-based maintenance of power-plant auxiliary motors.

2. METHOD

This study is a diagnostic case study using multi-parameter measurement on a single 6 kV Primary Air Fan induction motor during a scheduled overhaul. Four classes of tests were performed: two electrical (insulation resistance; winding resistance) and two mechanical (bearing vibration; mechanical clearance). Where a parameter admitted a meaningful before/after pairing, readings were taken both before and after the intervention, and each change is interpreted against the conditions under which the two readings were acquired; the overhaul work scope and the resulting test sequence are stated in Section 2.3, and the procedure for each parameter in Section 2.4. The procedure is organized as a staged assessment in which the output of each stage constitutes the admissible input of the next, so that no interpretation is made before the measurement conditions that license it have been established; staged evaluation frameworks of this kind, in which each phase is completed and validated before the following one begins, are used across engineering-assessment practice [23]. The overall research procedure, from object identification through standard-referenced evaluation to the quantification of overhaul effectiveness, is summarized in Figure 1.

Figure 1. Research flowchart of the multi-parameter diagnostic assessment of the 6 kV PA Fan motor.

2.1. Object of Study

The test object is a three-phase induction motor driving the PA Fan of Unit 2A at PLTU Pelabuhan Ratu: a machine rated 6300 V, which operates on a nominal 6 kV auxiliary system and is referred to throughout this article by that nominal class. At both ends the shaft is carried in a labyrinth-sealed bearing housing with an adjustable seat, which is the arrangement that defines the three clearance features measured in Section 2.4 — the labyrinth seal, the bearing top clearance, and the twist seat — and governs their interpretation in Section 3.4. Nameplate data are summarized in Table 1.

Table 1. Motor nameplate specification (Shanghai Electric YKK630-4TH)

Parameter	Value
Manufacturer / type	Shanghai Electric / YKK630-4TH
Rated power	2000 kW
Rated voltage	6300 V (6.3 kV)
Rated current	208 A
Poles / rated speed	4 poles / 1487 rpm
Frequency / phases	50 Hz / 3-phase
Power factor	0.922
Insulation class	F
Winding connection	Star (Y)
Protection degree	IP55
Serial no. / weight	630Y112118-1 / 10550 kg
Design standard	IEC 60034-1

Reference: motor nameplate data.

The motor drives the PA Fan in a 2 × 50% configuration and is supplied from the 6 kV auxiliary switchgear. At 2000 kW rated power (> 300 kW), it is classified as a Group 1 machine under ISO 20816-3 [14], which fixes the applicable vibration-zone boundaries used in Section 3.3.

2.2. Instrumentation

Table 2 lists each measured quantity together with the corresponding instrument model and its measurement range, resolution, or test setting. Insulation resistance was measured with a Megger MIT525 insulation tester at a DC test voltage of 5000 V, consistent with IEEE Std 43-2013 [5] for machines in this voltage class; the instrument covers 250–5000 V DC in 25 V steps, ranges to 10 TΩ, and performs automatic post-test discharge. Winding resistance was measured with a KRI 9310 digital low-resistance ohmmeter (DLRO) using the four-wire (Kelvin) method per IEEE Std 112-2017 [24] to eliminate lead-and-contact resistance, over a range of 0.1 μΩ to 2000 Ω with test current up to 10 A. Vibration was measured with an SKF Microlog CMXA 85 analyzer using an accelerometer mounted on the bearing housing, reporting RMS velocity in the three orthogonal directions. Mechanical clearance was measured with a stainless-steel feeler gauge (labyrinth), the lead-wire-and-micrometer method (bearing top clearance), and a dial indicator (the twist seat: the axial-locating seat of the bearing housing, whose left and right readings reveal any angular twist of the housing relative to the shaft axis). The resolutions listed in Table 2 fix the smallest change that can be regarded as a real measurement rather than an artifact: 0.01 mm for the micrometer-based bearing-top readings, the dial-indicator twist-seat readings, and the feeler-gauge labyrinth readings alike. Every clearance change discussed in Section 3.4 is therefore compared against these resolutions before being interpreted.

Table 2. Measurement instrumentation

Quantity	Instrument / model	Range / setting
Insulation resistance	Megger MIT525 insulation tester	5000 V DC; to 10 TΩ
Winding resistance	KRI 9310 DLRO (micro-ohmmeter)	4-wire; 0.1 μΩ–2000 Ω; ≤ 10 A
Vibration	SKF Microlog CMXA 85 analyzer	RMS velocity, 3-axis
Labyrinth clearance	Feeler gauge (stainless steel)	blade set 0.03–1.00 mm; increment 0.01 mm
Top / bearing clearance	Lead wire + micrometer screw	0–25 mm; resolution 0.01 mm
Twist seat	Dial indicator	resolution 0.01 mm

Reference: instrument manufacturer specifications.

2.3. Overhaul Work Scope and Test Sequence

The overhaul comprised disassembly and inspection of both bearing assemblies, cleaning of the stator winding and the ventilation passages, re-seating and re-adjustment of the bearing housings, re-cutting of the labyrinth seals, and reassembly followed by a no-load running test. No rewinding, coil replacement, or other electrical repair was carried out, and no rotor balancing was performed.

The test sequence follows from that scope and governs how the results in Section 3 must be read. Before the overhaul, the vibration readings were taken with the machine running under no-load and under load, immediately before shutdown, and the insulation-resistance test was performed afterwards on the cold, stationary machine. The bearing and seal clearances were then recorded during disassembly. After reassembly, the insulation-resistance test was performed immediately following the no-load running test and therefore on a warm winding, the winding-resistance measurement was taken in the same warm condition, the clearances were re-recorded on the reassembled machine, and the vibration readings were repeated under both no-load and load conditions.

2.4. Test Procedures

(a) Insulation resistance was measured winding-to-ground over 10 minutes, with values recorded at 30 s and then at 1-minute intervals to 10 min, from which the DAR (R1 min/R30 s) and PI (R10 min/R1 min) were derived. (b) Winding resistance was measured across the three phase pairs (U–V, U–W, V–W) in the warm condition immediately after operation; because no rewinding or winding repair was performed during the overhaul, no pre-/post-overhaul comparison exists for this parameter, and the measurement was instead repeated within the same session to check reading stability. (c) Vibration was measured on the drive-end (DE) and non-drive-end (NDE) bearings in the vertical, horizontal, and axial directions under two conditions: no-load (motor uncoupled) and load (coupled to the fan). (d) Clearance was measured with a feeler gauge on the labyrinth seals (inner/outer at Up/Down/Left/Right), with the lead-wire-and-micrometer method on the bearing top clearance (Positions 1 and 2), and with a dial indicator on the twist seat at the inner and outer left/right positions (OL, IL, IR, OR). Acceptance for all three clearance features follows the manufacturer design tolerances, with IEC 60034-1 [25] cited as the governing rating-and-performance framework for the machine.

2.5. Test Environment

Winding and ambient temperature and humidity were not recorded during testing. The analytical design adopted here follows directly from that measurement condition: because absolute insulation-resistance values cannot be normalized to the 40 °C reference of IEEE Std 43-2013, insulation integrity is assessed through the ratio-based relative indices defined in Section 2.6, which are formed from readings taken within a single test session and are therefore evaluated at a common winding temperature.

2.6. Data-Analysis Methods

Insulation condition was evaluated through the DAR and PI indices. The 1-minute insulation resistance normalized to 40 °C (≥ 100 MΩ for this machine rating) and the minimum PI of 2.0 for Class F insulation are the acceptance values given in IEEE Std 43-2013 [5]; the DAR criterion of 1.25 applied here is the conventional industry acceptance value, the standard itself tabulating PI rather than DAR. Because both readings forming each ratio are taken within a single test session at a practically constant winding temperature, these ratios are considerably less affected by the absolute test temperature than single-point resistance values. They are, nevertheless, not strictly temperature-independent: the absorption and polarization currents that determine DAR and PI are themselves temperature-dependent. The indices are therefore used here as supporting evidence rather than as temperature-corrected quantities; it is for this reason that IEEE Std 43-2013 requires the winding temperature to be recorded for every test [5], [26].

Winding-resistance unbalance was computed as the maximum deviation from the phase average, per Eq. (1). This maximum-deviation form follows the definition of percent unbalance given in NEMA MG 1 [27] and is retained here in preference to averaging the absolute per-phase deviations, because it is the worst phase that the acceptance limit governs. The ≤ 2% threshold applied to the winding-resistance unbalance is the plant acceptance criterion, consistent with established industry practice for this measurement; IEEE Std 112 is cited only for the winding-resistance measurement procedure [24].

$$Unbalance\ (\%) = (R_{max} - R_{avg}) / R_{avg} \times 100 \quad (1)$$

For reference, temperature correction of copper resistance follows Eq. (2). Because winding temperature was not recorded, this correction is not applied here, and the analysis relies on the relative inter-phase unbalance, which is unaffected by a uniform temperature elevation.

$$R_{ref} = R_{meas} \times (234.5 + T_{ref}) / (234.5 + T_{meas}) \quad (2)$$

Vibration severity was assessed against the four evaluation zones (A/B/C/D) of ISO 20816-3 [14], whose boundaries depend on the machine power group and the support class (rigid or flexible), as tabulated in Section 3.3. Clearance values were compared with the manufacturer design tolerances for this frame, within the rating-and-performance framework of IEC 60034-1 [25].

3. RESULTS AND DISCUSSION

The measured data are presented per parameter together with their interpretation against the applicable standards; the overall synthesis of overhaul effectiveness is given in Section 3.5.

3.1. Insulation Resistance

Table 3 reports the insulation-resistance measurements before and after the overhaul, with the derived DAR and PI indices. Every recorded value lies at least an order of magnitude above the 100 MΩ minimum, the lowest reading of the entire campaign being 1.10 GΩ. Figure 2 plots the two 10-minute absorption curves on a common time base, showing that both retain the monotonically rising profile characteristic of sound insulation, the post-overhaul curve lying roughly five- to eightfold lower across the 10-minute window (4.8× at 30 s, rising to 8.1× at 10 min).

Table 3. Insulation-resistance measurement (resistance values in GΩ; DAR and PI dimensionless)

Time (min)	Before (GΩ)	After (GΩ)
0.5 (30 s)	5.27	1.10
1	9.20	1.78
2	14.68	2.47
3	18.86	2.87
4	21.80	3.16
5	24.50	3.35
6	27.50	3.55
7	29.30	3.73
8	31.30	3.95
9	32.70	4.15
10	34.40	4.25
DAR	1.75	1.62
PI	3.74	2.39

Reference: IEEE Std 43-2013 — R (1 min, 40 °C) ≥ 100 MΩ and PI ≥ 2.0; DAR ≥ 1.25 per conventional industry practice.

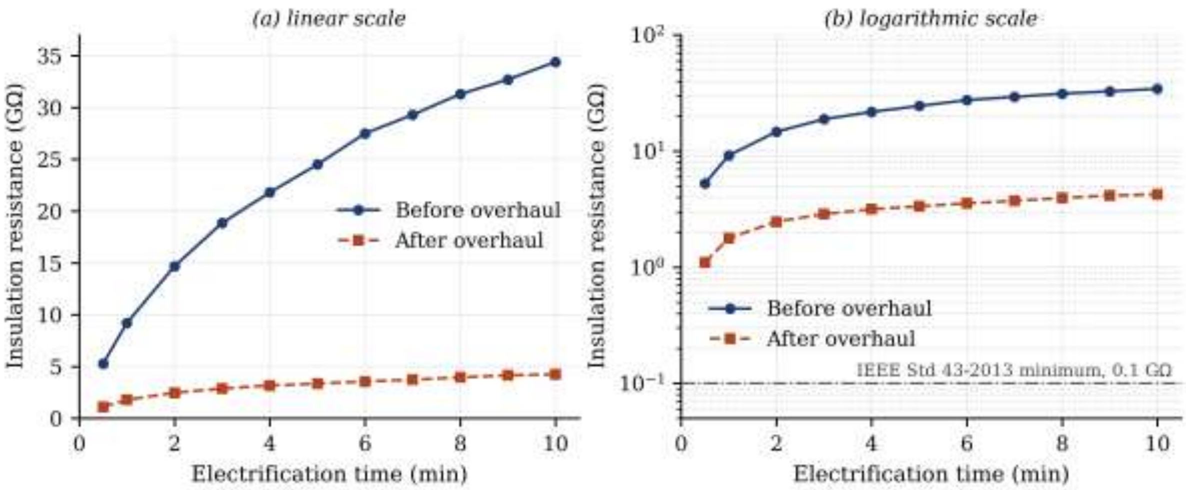

Figure 2. Insulation-resistance absorption curves before and after the overhaul (5000 V DC, 10 min), with the derived DAR and PI indices.

The decrease in absolute insulation resistance from 34.40 GΩ to 4.25 GΩ at the 10-minute mark is consistent with a measurement performed on a warm winding immediately after the no-load running test (Section 2.3), given the strong inverse dependence of insulation resistance on winding temperature [5], [6]. A separation of roughly five- to eightfold between the two curves is of the order expected from a winding tens of degrees above its pre-test state; the exact elevation cannot be recovered, because the winding temperature was not recorded and the correction factor for the thermosetting Class F insulation of this machine is machine-specific rather than given by the classical halving-per-10 °C rule [5]. This reversible temperature dependence of the measured resistance is a distinct phenomenon from the Montsinger thermal-aging rule, under which each 10 °C rise roughly halves insulation service life, and the two must not be conflated when a pre-/post-overhaul comparison is interpreted [6], [7]. Insulation integrity is accordingly established through the ratio-based relative indices: the post-overhaul DAR of 1.62 (> 1.25) and PI of 2.39 (> 2.0) both exceed their thresholds. The pre-overhaul PI (3.74) is not used as a criterion: the pre-overhaul 1-minute resistance, 9.20 GΩ as measured, is well above the 5 GΩ level beyond which IEEE Std 43-2013 states that PI ceases to be a reliable indicator, and the standard applies that screen to the resistance corrected to 40 °C, which cannot be formed here. The apparent decline in PI from 3.74 to 2.39 is therefore an artifact of the differing test conditions rather than an indication of dielectric degradation [5]. The insulation is therefore in good condition, and the motor is safe to operate from the standpoint of insulation resistance.

3.2. Winding Resistance

Table 4 reports the winding resistance across the three phase pairs. Because no winding repair was performed (Section 2.3), the two columns are repeat measurements taken in the warm post-operation condition within the same test session (not a pre-/post-overhaul comparison). The two sets are identical to the last displayed digit (1 μΩ) on all three phase pairs; the repeat acquisitions therefore resolved no change in either the winding resistance or the four-wire contact resistance over the acquisition interval.

Table 4. Winding-resistance measurement (warm condition; two repeat measurements)

Phase	Measurement 1 (mΩ)	Measurement 2 (mΩ)
U–V	217.134	217.134
U–W	216.625	216.625
V–W	217.788	217.788

Reference: unbalance ≤ 2% (plant acceptance criterion; unbalance defined per NEMA MG 1).

The inter-phase unbalance, computed with Eq. (1) as the maximum deviation from the phase average (R_{avg} = 217.182 mΩ, R_{max} = 217.788 mΩ), is 0.279%, far below the 2% acceptance limit. Because unbalance is a relative quantity among phases at the same temperature, this value is unaffected by the temperature elevation associated with the warm-condition measurement. The winding is therefore homogeneous with respect to DC resistance, with no indication of loose connections or contact-resistance unbalance. It must be emphasized, however, that a balanced DC winding resistance is not a valid basis for excluding turn-to-turn (inter-turn) insulation faults: a small number of shorted turns may alter the phase resistance by an amount comparable to the measurement uncertainty [28]. Detecting such faults requires a diagnostic that stresses the turn insulation directly, such as the surge comparison test [28]. The scope of the present winding-resistance result is therefore precisely bounded — it establishes inter-phase homogeneity and connection integrity — and surge comparison testing is identified as the complementary test that extends the assessment to the turn insulation.

3.3. Vibration

Table 5 reports the RMS velocity of the DE and NDE bearings in the vertical, horizontal, and axial directions under no-load and load conditions, before and after the overhaul.

Table 5. Bearing vibration measurement (RMS velocity, mm/s)

Condition	Bearing	Vert. Before	Vert. After	Horiz. Before	Horiz. After	Axial Before	Axial After
No load	DE	0.45	0.62	0.61	0.72	0.90	0.65
No load	NDE	0.77	0.66	0.83	0.54	0.72	0.87
Load	DE	2.32	1.27	1.75	1.84	3.24	2.43
Load	NDE	1.73	0.88	2.35	2.14	1.37	1.59

Reference: ISO 20816-3 (zone limits tabulated in Table 6).

ISO 20816-3 defines four evaluation zones (A/B/C/D) rather than a single threshold, and the zone boundaries depend on the machine power group and support class, as summarized in Table 6 [14]. Case studies on boiler draft fans evaluate the overall RMS velocity directly against these zone boundaries in the same way [29], [30]. A single 4.5 mm/s pass/fail threshold is often applied in plant practice; it corresponds specifically to the B/C boundary for a Group 1 machine on a rigid foundation. Correctly classifying the machine is therefore a prerequisite for interpreting the data.

Table 6. ISO 20816-3 evaluation-zone boundaries (RMS velocity, mm/s)

Classification	A/B	B/C	C/D
Group 1 (> 300 kW), rigid support	2.3	4.5	7.1
Group 1 (> 300 kW), flexible support	3.5	7.1	11.0
Group 2 (15–300 kW), rigid support	1.4	2.8	4.5

Reference: ISO 20816-3:2022.

At 2000 kW rated power (Table 1), the motor is a Group 1 machine (> 300 kW). ISO 20816-3 distinguishes rigid from flexible support by whether the first natural frequency of the machine–support system lies above the principal exciting frequency; that frequency was not determined in this campaign, so the machine was classified as rigidly supported, consistent with its mounting on a concrete foundation block. Because the flexible-support boundaries are the less restrictive of the two, the rigid classification is the conservative choice and the compliance conclusion holds under either. On that basis all load-condition values fall within Zones A–B (acceptable). Three before-overhaul values exceed the A/B boundary of 2.3 mm/s and therefore lie in Zone B rather than the "as-new" Zone A: DE axial (3.24 mm/s), NDE horizontal (2.35 mm/s), and DE vertical (2.32 mm/s). After the overhaul only DE axial, at 2.43 mm/s, remains above that boundary, and it is therefore the single point carried forward for trend monitoring. This correct classification is essential: had the motor been treated as Group 2 (15–300 kW), the DE axial value of 3.24 mm/s would fall in Zone C, which ISO 20816-3 describes as normally considered unsatisfactory for long-term continuous operation, which is why the single ≤ 4.5 mm/s "good" threshold — valid only as the Group 1 rigid-support B/C boundary — must be replaced by the full zone table.

The effectiveness of the overhaul is quantified per measurement point under load in Table 7 and displayed against the Group 1 rigid-support zone boundaries in Figure 3. The average load-condition vibration fell from 2.13 to 1.69 mm/s, a 20.5% reduction. The improvement is largest in the vertical direction (−45.3% at DE and −49.1% at NDE), with a further 25.0% reduction in DE axial, whereas the horizontal direction shows a mixed response. A predominantly vertical improvement is the response expected from a bearing-clearance correction on a horizontally mounted machine, since the static gravity load is carried in that plane and it is there that excess clearance most directly permits shaft excursion [12], [31]. Figure 3 also makes visible that the two points that increased (DE horizontal, 1.84 mm/s; NDE axial, 1.59 mm/s) remain within Zone A, so the mixed directional response does not alter the severity classification of the machine. Under no-load, the absolute values span 0.45–0.90 mm/s, roughly a third of the load-condition levels, and lie deep within Zone A, so the dynamic forces that the overhaul acted upon are not excited in that condition; the no-load changes are therefore not interpreted as improvements. This load-versus-no-load contrast reinforces the conclusion that the benefit of the overhaul manifests when dynamic forces are excited under load.

Table 7. Quantified change in load-condition vibration (after vs. before)

Point (load)	Before (mm/s)	After (mm/s)	Change
DE Vertical	2.32	1.27	−45.3%
DE Horizontal	1.75	1.84	+5.1%
DE Axial	3.24	2.43	−25.0%
NDE Vertical	1.73	0.88	−49.1%
NDE Horizontal	2.35	2.14	−8.9%
NDE Axial	1.37	1.59	+16.1%
Load-condition average	2.13	1.69	−20.5%

Reference: computed from the load-condition rows of Table 5.

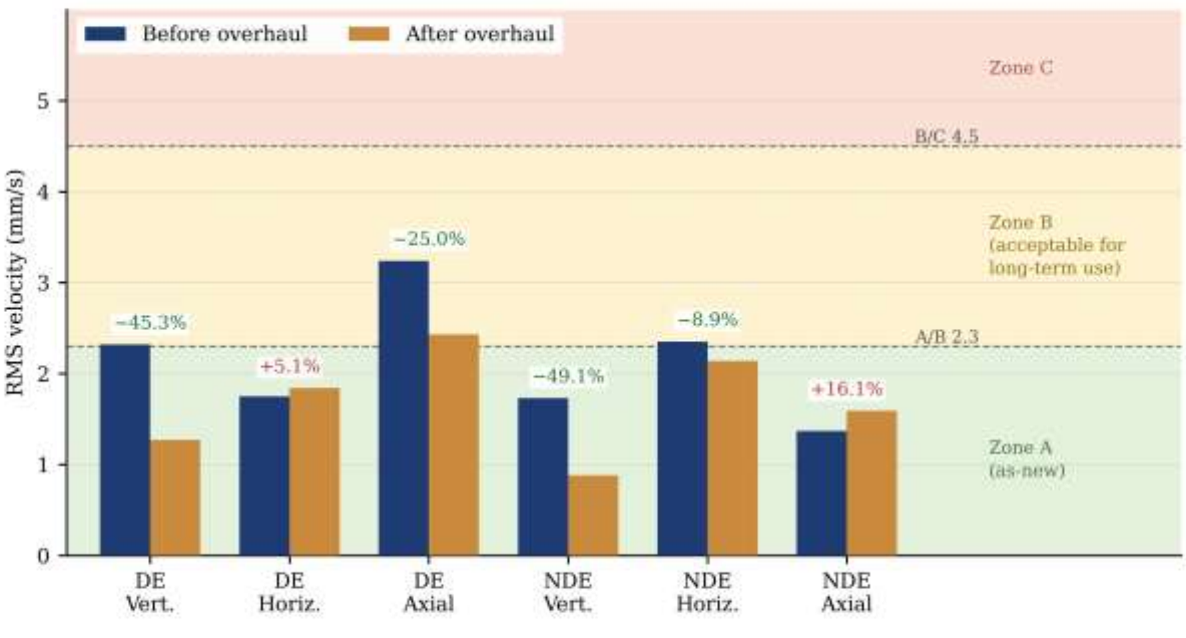

Figure 3. Load-condition RMS velocity before and after the overhaul at the six measurement points, referenced to the ISO 20816-3 Group 1 rigid-support zone boundaries (A/B = 2.3 mm/s; B/C = 4.5 mm/s).

Because each point is a single unreplicated reading rather than a repeated sample, no inferential statistics (e.g., t-tests or p-values) are applied; doing so would be statistically unsound in the absence of an intra-condition variance estimate. The analysis is therefore reported as descriptive effect magnitudes together with the ISO 20816-3 zone classification.

3.4. Mechanical Clearance

Tables 8–10 report the labyrinth-seal clearance, bearing top clearance, and twist-seat clearance, before and after the overhaul, referenced to IEC 60034-1 [25].

Table 8. Labyrinth-seal clearance (mm)

Position	Point	Inner Before	Inner After	Outer Before	Outer After
DE	Up	0.15	0.15	0.08	0.10
DE	Down	0.00	0.05	0.00	0.05
DE	Left	0.03	0.07	0.09	0.07
DE	Right	0.00	0.08	0.03	0.08
NDE	Up	0.10	0.15	0.10	0.10
NDE	Down	0.00	0.05	0.00	0.05
NDE	Left	0.03	0.07	0.08	0.07
NDE	Right	0.05	0.08	0.03	0.08

Reference: manufacturer design tolerances, within the IEC 60034-1 framework.

Table 9. Bearing top clearance (mm)

Bearing	Position 1 (Before / After)	Position 2 (Before / After)
DE	0.20 / 0.19	0.19 / 0.20
NDE	0.19 / 0.23	0.32 / 0.22

Reference: IEC 60034-1 and manufacturer design tolerances.

Table 10. Twist-seat clearance (mm), inner (IL, IR) and outer (OL, OR) positions

Position	Point	Before	After
DE	OL	0.10	0.10
DE	IL	0.10	0.10
DE	IR	0.12	0.10
DE	OR	0.11	0.10
NDE	OL	0.11	0.10
NDE	IL	0.00	0.11
NDE	IR	0.00	0.11
NDE	OR	0.11	0.11

Reference: IEC 60034-1 and manufacturer design tolerances.

IEC 60034-1 governs the rating and performance of the machine but does not tabulate feature-specific numeric limits for labyrinth seals or bearing seats. The measured values span 0.00–0.32 mm. Acceptance for the three clearance families reported here therefore follows the manufacturer design tolerances for this frame, with IEC 60034-1 providing the surrounding framework rather than the numeric criterion.

Interpreted in relation to the vibration behavior, the most diagnostically significant change is the sharp reduction of the NDE top clearance at Position 2, from 0.32 to 0.22 mm after the overhaul (Table 9), which is the direct signature of the NDE bearing re-seating carried out during the overhaul (Section 2.3). The 0.10 mm reduction is ten times the 0.01 mm resolution of the lead-wire-and-micrometer method (Table 2) and is therefore a physically real change rather than a reading artifact, in contrast to the ±0.01 mm variations seen at the two DE positions, which are at the resolution limit and carry no diagnostic weight. The same resolution criterion admits a second real change in Table 9, the increase at NDE Position 1 from 0.19 to 0.23 mm (0.04 mm, four times the resolution); taken together with the reduction at Position 2, the two readings describe a re-seating that equalized the NDE bearing clearance from a 0.19/0.32 mm asymmetry to a nearly uniform 0.23/0.22 mm, which is the physically meaningful outcome rather than either reading in isolation. This equalization coincides with the 49.1% reduction in NDE vertical vibration under load (1.73 → 0.88 mm/s), and is the mechanism that rotor–bearing dynamics predicts for it, indicating that the mechanical clearance correction — rather than any electrical action — was the principal contributor to the improved dynamic performance of the motor. The direction of this correlation is the one predicted by rotor–bearing dynamics: an enlarged radial clearance increases the free radial excursion of the shaft before the bearing re-establishes the load path, which raises the vibration amplitude transmitted to the housing, whereas restoring the clearance toward the design fit suppresses it [31]. Root-cause investigations of bearing failures report the same coupling between bearing seating condition and measured housing vibration [11], and case studies on draft fan rotors show that the corresponding correction is observable directly in the overall RMS velocity [30].

A consistent pattern runs through the twist-seat and labyrinth data: every 0.00 mm entry in Tables 8 and 10 — the two NDE twist-seat positions IL and IR, and five labyrinth points at the Down and Right positions — became a finite clearance after the overhaul, in the range 0.05 to 0.11 mm. On a dial indicator and on a feeler gauge alike, a 0.00 mm reading denotes seating with no measurable gap. Four of the five labyrinth zeros occur at the gravity-loaded Down position, which is consistent with a settled rotor; the two zero twist-seat readings, at the opposed inner-left and inner-right seats, instead indicate no measurable play at the inner seat itself. In both cases the restoration of a finite clearance is the intended outcome of the work: it removes the local pre-load and the associated risk of seal rub, and the resulting values lie within the manufacturer design tolerances for this frame. Across the labyrinth seals the summed diametral clearance also increased at every station, indicating that the seals were re-cut during the overhaul rather than merely re-centered. The remaining individual labyrinth changes span zero to five times the 0.01 mm feeler increment and are not interpreted point by point in the absence of repeat readings.

3.5. Synthesis of Overhaul Effectiveness

Taken together, the overhaul delivered a measurable mechanical improvement — a 49.1% reduction in load-condition vibration in the vertical direction at the NDE, correlated with the correction of the NDE bearing clearance — whereas the electrical parameters were sound: the insulation met its criteria in both test sessions when interpreted through ratio-based indices, and the winding resistance measured after the work showed an inter-phase unbalance far inside the acceptance limit. The study therefore quantifies that the principal value added by the overhaul on this motor was mechanical, and it shows why the temperature normalization required by IEEE Std 43-2013 must be observed if the electrical parameters are not to be misdiagnosed. This reframes the assessment from a binary declaration of fitness toward a quantified account of how much, and through which mechanism, the overhaul acted. Framed in condition-based maintenance terms, the result also identifies which measurement channel carried the diagnostic information on this machine: the load-condition vertical vibration and the bearing top clearance are the pair that responded to the intervention, and are therefore the pair proposed for trending between overhauls, subject to confirmation on further units [15].

4. CONCLUSION

This study evaluated a 6 kV Primary Air Fan induction motor through multi-parameter diagnostics during a scheduled overhaul, with three principal findings. First, the overhaul produced a measurable mechanical improvement: load-condition vibration fell by 20.5% on average, with a reduction of 49.1% in the vertical direction at the non-drive-end bearing that correlates directly with the equalization of the NDE bearing top clearance (0.19/0.32 → 0.23/0.22 mm), indicating that the dominant benefit of the overhaul for this motor was mechanical. Second, the electrical parameters were sound: the winding-resistance unbalance was 0.279% (well below the 2% acceptance limit), and the insulation was confirmed as sound through the ratio-based DAR (1.62) and PI (2.39) indices, while the post-cleaning drop in absolute insulation resistance was consistent with measurement on a warm winding rather than with dielectric degradation. Third, every measured parameter complies with its applicable acceptance criterion: vibration lies within Zones A–B of ISO 20816-3 for a Group 1 machine on a rigid support; insulation and winding resistance satisfy IEEE Std 43-2013 and the ≤ 2% unbalance criterion; and the labyrinth, bearing-top, and twist-seat clearances lie within the manufacturer design tolerances, IEC 60034-1 being cited as the governing rating-and-performance framework for the machine although it does not itself tabulate feature-specific numeric limits for these clearances. The motor is therefore fit for continued operation. The main contribution of this article is to document, on field data, the consequence of omitting the temperature normalization that IEEE Std 43-2013 requires for pre-/post-overhaul comparison of insulation resistance: without it, a correct maintenance action can be misread as dielectric degradation.

The scope of these findings is defined by the design of the study. It is a single-unit field case, so the numerical effect magnitudes reported here characterize this machine and this intervention; extending them to a machine class requires replication across a population, which is the natural next step for this framework. Each parameter is a single unreplicated reading per condition, with winding resistance repeated within the session, so the results are reported as descriptive effect magnitudes against standard-defined acceptance zones — the form of evidence that standards-based acceptance testing is designed to produce. Because winding temperature was not recorded, absolute insulation resistance is not normalized to 40 °C, and insulation integrity is established instead through the ratio-based DAR and PI indices, which are formed within a single test session at a common winding temperature and are for that reason the appropriate instrument here.

Future work should include long-term trend monitoring of load-condition vibration and temperature-normalized insulation resistance to establish the degradation rate; integration of Motor Current Signature Analysis (MCSA) for the early detection of rotor faults not reachable by offline testing [8]; and replication of the multi-parameter assessment framework across a population of auxiliary motors to build a generalizable condition-based maintenance database.

ACKNOWLEDGMENTS

The authors thank the management and maintenance engineers of PLTU Pelabuhan Ratu for facilitating field access during the scheduled overhaul, and the Professional Engineer Program, Universitas Pendidikan Indonesia, for academic support.

REFERENCES

[1] H. Satria, A. T. Feriyanto, A. R. Hasan, and A. Kurniawan, “New utilisation of subcritical coal-fired power plant in Indonesia: Case study of flexible power plant hot test at PLTU Pelabuhan Ratu (300 MW CFPP),” in *Proc. 2025 5th Int. Conf. High Voltage Eng. Power Syst. (ICHVEPS)*, Denpasar, Indonesia, 2025, doi: 10.1109/ICHVEPS66913.2025.11351135.

[2] A. Pambudi, I. Sukmana, and Y. Risano, “Pengaruh nilai spesifik konsumsi bahan bakar (SFC) terhadap jumlah pemakaian batubara di PT Bukit Energi Servis Terpadu PLTU Peltar 2×8 MW” (in Indonesian), *Jurnal Profesi Insinyur Universitas Lampung*, vol. 4, no. 2, pp. 133–142, 2023, doi: 10.23960/jpi.v4n2.109.

[3] Z. Kłosowski, M. Fajfer, and Z. Ludwikowski, “Reduction of the electromagnetic torque oscillation during the direct on line (DOL) starting of a 6 kV motor by means of a controlled vacuum circuit-breaker,” *Energies*, vol. 15, no. 12, art. no. 4246, 2022, doi: 10.3390/en15124246.

[4] M. Dems, K. Majer, and K. Komęza, “Optimization of induction motor control to limit the maximum current and torque during voltage start-up using FEM and analytical simulation,” *Energies*, vol. 19, no. 1, art. no. 240, 2026, doi: 10.3390/en19010240.

[5] *IEEE Recommended Practice for Testing Insulation Resistance of Electric Machinery*, IEEE Std 43-2013 (Revision of IEEE Std 43-2000), IEEE, Piscataway, NJ, USA, 2014, doi: 10.1109/IEEESTD.2014.6754111.

[6] B. Sirizzotti, D. Addae, E. Agamloh, A. von Jouanne, and A. Yokochi, “A review of stator insulation state-of-health monitoring methods,” *Energies*, vol. 18, no. 14, art. no. 3758, 2025, doi: 10.3390/en18143758.

[7] D. Addae and E. Agamloh, “A review of electric machine stator winding insulation diagnostic signal processing methods and metrics,” *Machines*, vol. 14, no. 7, art. no. 751, 2026, doi: 10.3390/machines14070751.

[8] K. Hamani, M. Kuchar, M. Kubatko, and S. Kirschner, “Advancements in induction motor fault diagnosis and condition monitoring: A comprehensive review,” *Sensors*, vol. 25, no. 19, art. no. 5942, 2025, doi: 10.3390/s25195942.

[9] G. Niu, X. Dong, and Y. Chen, “Motor fault diagnostics based on current signatures: A review,” *IEEE Trans. Instrum. Meas.*, vol. 72, pp. 1–19, 2023, doi: 10.1109/TIM.2023.3285999.

[10] R. R. Kumar, M. Andriollo, G. Cirrincione, M. Cirrincione, and A. Tortella, “A comprehensive review of conventional and intelligence-based approaches for the fault diagnosis and condition monitoring of induction motors,” *Energies*, vol. 15, no. 23, art. no. 8938, 2022, doi: 10.3390/en15238938.

[11] D. Tahmasbi, H. Shirali, S. S. Mousavi Nejad Souq, and M. Eslampanah, “Diagnosis and root cause analysis of bearing failure using vibration analysis techniques,” *Eng. Failure Anal.*, vol. 158, art. no. 107954, 2024, doi: 10.1016/j.engfailanal.2023.107954.

[12] B. Wu and M. Qiao, “A review of the research progress of motor vibration and noise,” *Int. Trans. Electr. Energy Syst.*, vol. 2022, art. no. 5897198, 2022, doi: 10.1155/2022/5897198.

[13] M. Pandiyan and T. N. Babu, “Systematic review on fault diagnosis on rolling-element bearing,” *J. Vib. Eng. Technol.*, vol. 12, no. 7, pp. 8249–8283, 2024, doi: 10.1007/s42417-024-01358-4.

[14] *Mechanical Vibration — Measurement and Evaluation of Machine Vibration — Part 3: Industrial Machinery with a Power Rating Above 15 kW and Operating Speeds Between 120 r/min and 30 000 r/min*, ISO 20816-3:2022, International Organization for Standardization, Geneva, Switzerland, 2022.

[15] A. Nazarychev, I. Iliev, D. Manukian, H. Beloev, K. Suslov, and I. Beloev, “Review of operating conditions, diagnostic methods, and technical condition assessment to improve reliability and develop a maintenance strategy for electrical equipment,” *Energies*, vol. 18, no. 21, art. no. 5832, 2025, doi: 10.3390/en18215832.

[16] A. Ali and A. Abdelhadi, “Condition-based monitoring and maintenance: State of the art review,” *Appl. Sci.*, vol. 12, no. 2, art. no. 688, 2022, doi: 10.3390/app12020688.

[17] M. Moleda, B. Małysiak-Mrozek, W. Ding, V. Sunderam, and D. Mrozek, “From corrective to predictive maintenance — A review of maintenance approaches for the power industry,” *Sensors*, vol. 23, no. 13, art. no. 5970, 2023, doi: 10.3390/s23135970.

[18] S. Supratno and M. Khairudin, “An integrated SCADA–PLC–HMI model for low-cost control and real-time monitoring of three-phase AC motors,” *Jurnal Nasional Teknik Elektro*, vol. 14, no. 3, pp. 181–189, 2025, doi: 10.25077/jnte.v14n3.1298.2025.

[19] R. Irwanto, A. Asep, and H. Hermawan, “Metoda sederhana untuk memperbaiki kinerja motor listrik 3 fasa berdasarkan insulation resistance test” (in Indonesian), *Jurnal Pengelolaan Laboratorium Pendidikan*, vol. 6, no. 1, pp. 55–62, 2024, doi: 10.14710/jplp.6.1.55-62.

[20] K. R. Butukuri, N. C. Giri, P. K. Yemula, R. K. K. R. Penubaka, H. Vennila, and S. R. Das, “Assessment of a 40-year-old induction motor using hybrid diagnostic and AI-based predictive techniques,” *Sci. Rep.*, vol. 16, art. no. 13739, 2026, doi: 10.1038/s41598-026-44319-5.

[21] B. A. Wokoma and K. Q. Blue-Jack, “Price-incentive distribution grid load scheduling using hybrid grey wolf optimization,” *JEECOM: J. Electr. Eng. Comput.*, vol. 8, no. 2, pp. 1–8, 2026, doi: 10.33650/jeecom.v8i2.16815.

[22] Alamsyah, A. Mustari, M. I. F. Rahman, and M. Ikhlayel, “Development and field evaluation of a solar-powered LoRa-based air quality monitoring and early-warning system for a sand-mining area,” *JEECOM: J. Electr. Eng. Comput.*, vol. 8, no. 2, pp. 36–47, 2026, doi: 10.33650/jeecom.v8i2.17080.

[23] L. Lisana, M. Angga, and E. C. Cristabella, “Enhancing user experience in a land transportation information application: A design thinking approach to the GOBIS application,” *JEECOM: J. Electr. Eng. Comput.*, vol. 8, no. 2, pp. 26–35, 2026, doi: 10.33650/jeecom.v8i2.16994.

[24] *IEEE Standard Test Procedure for Polyphase Induction Motors and Generators*, IEEE Std 112-2017 (Revision of IEEE Std 112-2004), IEEE, Piscataway, NJ, USA, 2018, doi: 10.1109/IEEESTD.2018.8291810.

[25] *Rotating Electrical Machines — Part 1: Rating and Performance*, IEC 60034-1:2022, International Electrotechnical Commission, Geneva, Switzerland, 2022.

[26] A. Decner, M. Barański, T. Jarek, and S. Berhausen, “Methods of diagnosing the insulation of electric machines windings,” *Energies*, vol. 15, no. 22, art. no. 8465, 2022, doi: 10.3390/en15228465.

[27] *Motors and Generators*, NEMA MG 1-2021, National Electrical Manufacturers Association, Rosslyn, VA, USA, 2021.

[28] L. A. Trujillo Guajardo, L. H. Rodriguez Alfaro, J. Rodriguez Maldonado, M. A. Gonzalez Vazquez, F. Salinas Salinas, and M. Y. Shih, “Prony method estimation as a new approach for surge comparison testing in turn insulation diagnostics for three phase stator windings,” *Machines*, vol. 11, no. 2, art. no. 241, 2023, doi: 10.3390/machines11020241.

[29] L. S. Dhamande, "Condition monitoring of forced-draft fan using vibration analysis: A case study," *Eng. Proc.*, vol. 93, no. 1, art. no. 9, 2025, doi: 10.3390/engproc2025093009.
[30] E. A. González-Barbosa, J. J. Vázquez-Martínez, F. Jurado-Pérez, H. Castro-Mosqueda, F. J. Rodríguez-Ornelas, and J.-J. González-Barbosa, "Analysis, modeling, and simulation solution of induced-draft fan rotor with excessive vibration: A case study," *Ingeniería e Investigación*, vol. 44, no. 2, art. no. e111284, 2024, doi: 10.15446/ing.investig.111284.
[31] H. Xu, P. Wang, H. Ma, Y. Yang, X. Li, Z. Luo, Q. Han, and B. Wen, "Dynamic behaviors and contact characteristics of ball bearings in a multi-supported rotor system under the effects of 3D clearance fit," *Mech. Syst. Signal Process.*, vol. 196, art. no. 110334, 2023, doi: 10.1016/j.ymssp.2023.110334.